CARBON 50 (2012) 896–905

Available at www.sciencedirect.com

SciVerse ScienceDirect

journal homepage: www.elsevier.com/locate/carbon

Synthesis, morphology and physical properties of multi-walled carbon nanotube/biphenyl liquid crystalline epoxy composites

Sheng-Hao Hsu [a], *Ming-Chung Wu* [b], *Sharon Chen* [b], *Chih-Min Chuang* [c], *Shih-Hsiang Lin* [b], *Wei-Fang Su* [a,b,*]

[a] *Institute of Polymer Science and Engineering, National Taiwan University, Taipei 10617, Taiwan*
[b] *Department of Materials Science and Engineering, National Taiwan University, Taipei 10617, Taiwan*
[c] *Institute of Nuclear Energy Research, Atomic Energy Council (AEC), Taoyuan 32546, Taiwan*

ARTICLE INFO

Article history:
Received 4 July 2011
Accepted 26 September 2011
Available online 2 October 2011

ABSTRACT

We have developed multi-walled carbon nanotube/liquid crystalline epoxy composites and studied the effects of incorporation carbon nanotubes (CNTs) on the morphology, thermal and mechanical properties of the composites. The CNTs are functionalized by liquid crystalline (LC) 4,4′-bis(2,3-epoxypropoxy) biphenyl (BP) epoxy resin for the ease of dispersion and the formation of long range ordered structure. The epoxy functionalized CNT (ef-CNT) were dispersed in the LC BP epoxy resin that can be thermal cured with an equivalent of 4,4′-diamino-diphenylsulfone to form composite. The curing process was monitored by polarized optical microscopy. The results indicate the LC resin was aligned along the CNTs to form fiber with dendritic structure initially then further on to obtain micro-sized spherical crystalline along with fibrous crystalline. With homogeneous dispersion and strong interaction between nanotubes and matrix, the composite containing 2.00 wt.% ef-CNT exhibits excellent thermal and mechanical properties. When the amount of ef-CNT exceeds 2.00 wt.%, vitrification stage of curing is fast reached, which lowers the degree of conversion. As compared with the neat resin, the composite containing 2.00 wt.% ef-CNT increases the glass transition temperature by 70.0 °C, the decomposition temperature by 13.8 °C, the storage modulus by 40.9%, and the microhardness by 63.3%.

1. Introduction

Composites that contain nanosized fillers have recently attracted a great deal of research interests. This is because their properties derive synergistically from the interactions among the components. Among all types, carbon nanotubes (CNTs)/polymer would be one of the most potential composite system for aerospace and many other industrial fields [1–6]. CNTs are found to have unique structural arrangement of atoms, high aspect ratio and excellent mechanical, thermal and electrical properties, making them ideal reinforcing components in host polymer matrices [7–10]. Additionally, CNTs are highly flexible. This property confers remarkable advantages to CNTs over conventional carbon fibers in composite processing [8]. Thus, researchers have shown great interest in using CNTs for high performance composite applications.

* *Corresponding author at:* Institute of Polymer Science and Engineering, National Taiwan University, Taipei 10617, Taiwan. Fax: +886 2 33664078.
E-mail address: suwf@ntu.edu.tw (W.-F. Su).
0008-6223/$ - see front matter
doi:10.1016/j.carbon.2011.09.051

The incorporation of CNTs into epoxy resins not only improves the electrical, thermal and mechanical properties of epoxy resins but also modifies their processing behaviors [2,11–14].

Liquid crystalline (LC) epoxy resin containing mesogenic rigid rod segment can form high crystalline domains under certain conditions. The mesogen groups of LC epoxy resin can align along a specific direction and then the epoxy functionality can be crosslinked to fix the alignment between chains to form self-reinforcing composite materials. Therefore, mesogen aligned and crosslinked LC epoxy resins offer better thermal and mechanical properties than that of conventional epoxy resin [15–21]. However, to obtain long range order aligned mesogen groups for further improved thermal and mechanical properties, researchers have explored using rather extreme magnetic field that requires precisely controlled temperature [22–24]. However, LC epoxy resins can be further reinforced by a second phase, and the alignment of the mesogen phase of LC epoxy is expected to be enlarged and elongated due to the presence of high aspect ratio second phase, such as CNTs. Therefore, it is possible to fabricate a composite possessing high mechanical properties, good thermal stability and electrical conductivity for aeronautic and astronautic engineering by utilizing both LC epoxy resin and CNTs. To date, there are very few reports of this type of composite [25].

CNTs are difficult to be dispersed into a polymer matrix due to strong van der Waal force is induced by the tremendous surface area of CNTs, which leads CNTs to bundle and aggregate together. For efficient reinforcement, the strong interfacial interaction between CNTs and the matrix is necessary to contribute the efficient load transfer from the matrix to CNTs. Many studies have demonstrated the application of chemical modification to the nanotubes can effectively improve the dispersion of CNTs in polymer matrix and therefore improve the physical properties of the composites [1–5,10].

We have developed a method for grafting LC epoxy functional groups onto the surface of CNTs. This allows functionalized CNTs to be easily dispersed into the LC epoxy resin. Then, the LC epoxy resin containing functionalized CNTs further reacts with curing agent to form a high performance composite. The resin system is made of 4,4′-bis(2,3-epoxypropoxy) biphenyl (BP) LC epoxy resin and 4,4′-diaminodiphenylsulfone (DDS) curing agent. The thermal and mechanical properties of the cured composites are examined with thermomechanical analysis (TMA), thermogravimetric analysis (TGA), dynamic mechanical analysis (DMA) and microhardness testing. The fibrous and spherical microstructures of cured composite were observed by polarized optical microscope (POM), scanning electron microscope (SEM) and transmission electron microscope (TEM). Incorporating functionalized CNTs into the LC resin system induces the formation of crystalline phase in the composite, thus greatly enhances the thermal and mechanical properties of the composite as compared with the neat LC epoxy resin system. Furthermore, the incorporation of thermal conductive CNT has accelerated the curing reaction of epoxy resin [26]. However, the excessive amount of CNT in matrix has resulted in reaching vitrification stage quickly and lowering the degree of conversion. We have observed the mechanical properties are decreased when the amount of CNT is >2.00 wt.%.

2. Experimental

2.1. Materials

The multi-walled carbon nanotubes (MWCNTs) were purchased from DESUN Nano Company (Taiwan) with an average diameter of ~20–30 nm, length of ~15 μm. The curing agent, diamino diphenyl sulfone was purchased from Acros. The LC epoxy resin, 4,4′-bis(2,3-epoxypropoxy) biphenyl was synthesised as previous described [15]. Typically, 22.00 g 4,4′-dihydroxybiphenyl was mixed with 190.0 ml epichlorohydrin and 0.82 g benzyltrimethylammonium bromide as a catalyst in a 500.0 ml 3-necked round bottom flask equipped with a 24/40 ground joint, a reflux condenser, and a magnetic stir-bar. Nitrogen purges for 30 min prior to the reaction to ensure the whole system was under an inert environment. The solution was heated to 120 °C and refluxed for 40 min until the solution appeared clear. Next, 15 wt.% NaOH solution (360.0 ml) was injected into the solution flask at a constant rate of 2.0 ml/min by using a programmable dispenser. After injecting the NaOH solution, the solution was cooled to room temperature and stirred for one more hour to allow the unreacted NaOH to react with epichlorohydrin. We obtained white precipitates of BP epoxy resin that floated in the solution. The precipitates were collected by filtration through 1 μm filter paper and then purified by rinsing with water and methanol respectively. Finally, the collected precipitates were dried in a vacuum oven overnight to obtain a white powder of BP epoxy resin with a melting point of 154 °C. The product has an epoxy equivalent weight of 180 g/mole according to the HCl-pyridine titration.

2.2. CNTs functionalization

4.00 g pristine CNT (p-CNT) was added into a 400.0 ml mixture of HNO_3:H_2SO_4 (volume ratio = 1:3). The p-CNT containing mixture was refluxed at 80 °C for 6 h and cooled to room temperature before it was diluted with distilled water 1:5 by volume. The solution was then filtered with the polytetrafluoroethylene (PTFE) filter of 0.2 μm pore size to collect the acid washed p-CNT. After collection, the acid washed p-CNT was rinsed with excess water and then dried at 105 °C for 24 h. Thus, acid modified CNT (a-CNT) was then obtained. Further functionalization was carried out by esterification between a-CNT and BP epoxy resin.

2.00 g a-CNT and 3.00 g BP epoxy resin were dispersed in 200.0 and 300.0 ml tetrahydrofuran (THF) respectively and then ultrasonicated in a 100 W bath sonicator for one hour at room temperature. After mixing the two solutions and ultrasonicating for an additional hour, 8.96 g KOH was added into the solution as a catalyst before the solution was refluxed at 70 °C for 6 h. The epoxy functionalized CNT (ef-CNT) were collected by filtration with PTFE filter and then dried as black powder. p-CNT, a-CNT and ef-CNT were characterized by using Fourier transform infrared spectrometer (JASCO FT/IR-480 Plus), and transmission electron microscope (JOEL JEM-1230).

2.3. Preparation of composites

1.50 g BP epoxy resin and required amount of ef-CNT (0.50, 1.00, 2.00, 4.00 and 10.00 wt.% ef-CNT, respectively) were dispersed in 20 ml THF. The solutions of mixtures were then ball milled for 48 h using zirconia milling balls. After ball milling, a 60 mesh sieve was used to separate the solution from zirconia milling ball. The solvent was removed by a rotary evaporator and the obtained gray powder product was vacuum-dried overnight.

2.4. Preparation of bulk composite samples

The composites with different ef-CNT compositions were prepared by mixing ef-CNT, BP epoxy resin and curing agent, DDS, based on the epoxide equivalent weight ratio of BP:DDS = 180:62. 1.00 g of the composite mixture was put into a 2×2 cm square mold and heated under a pressure of 245.38 kg/cm^2. The curing cycles of composite samples were set at 180 °C/12 h, 220 °C/10 h and post cure 250 °C/8 h. For the DMA measurement, the samples were cured at 180 °C/48 h, 220 °C/10 h and 250 °C/8 h. The surface of the cured samples was further polished with sandpaper of 800, 1000, and 2000 grits respectively, yielding samples have a thickness of ~2 mm.

2.5. Characterization of the bulk composites

For TEM observation, the cured samples were microtomed into 100 nm slices and then the TEM images were taken with a JEOL 1230 microscope operated at an accelerating voltage of 100 kV. The cured samples for SEM observation were fractured into small chunks and stuck onto a holder using carbon tape. The SEM images of the fractured samples were taken by using a JOEL JSM-6700F field emission scanning electron microscope at an accelerating voltage of 7.5 kV. The SEM samples were coated with platinum for better conductivity before viewing.

A TA instruments TGA 2950 was used to probe the thermal stability of the composites. 10–15 mg of the cured samples was weighed in a platinum pan. The experiments were performed from 30 to 600 °C at a rate of 10 °C/min under N_2. A TA instruments TMA 2940 was used to measure the dimensional changes in micro-scale. The experiments were performed from 30 to 300 °C at a rate of 10 °C/min under N_2. The cured samples were trimmed into a dimension of $5 \times 20 \times 2$ mm for measuring the mechanical properties by using a TA instruments Q800. The experimental conditions were set at 3-point bending mode, 1 Hz frequency, and 0.44 mm amplitude. The experiments were carried out from 30 to 300 °C at a rate of 2 °C/min under N_2. A HMV Micro Hardness Tester equipped with a Vickers diamond probe was used to determine the hardness in micro-scale. These tests were conducted with the loading force of 0.5 kg and a loading time of 10 s.

A Leica DM 2500 M microscope equipped with a cross polarizer, a digital camera (Leica DFC 420 C), and a Linkam CSS450 optical shearing system were used to image the LC phase of the epoxy resins during the heating process. Thin film resin samples were pressed between glass slides and the experiment was performed in air. For both the neat BP epoxy resin and 2.67 wt.% ef-CNT/BP, samples were heated at a rate of 2 °C/min until the samples melted at 165 °C. This temperature was held until the samples completely melted (about 30 min). Then the samples were cooled to room temperature at a rate of 0.5 °C/min. As the birefringence appeared at 162 °C, the temperature was held for observation. For BP/DDS resin system, the melting and observation temperatures were 140 and 137 °C, respectively. The crystalline structures of both cured thin film and bulk samples were observed after curing process.

3. Results and discussion

3.1. BP/DDS resin system for the matrix of composite

The LC epoxy resin, BP was blended with an equivalent curing agent of DDS to make the matrix of the composite. DDS was chosen because it is commonly used in high performance epoxy based composite [27]. Fig. 1 shows the chemical structure of each component in the matrix.

3.2. CNT functionalization

Functionalizing CNTs has been shown to enhance homogeneous dispersion of CNTs in various organic solvents and polymer matrices [1,28]. We have thus modified the surface

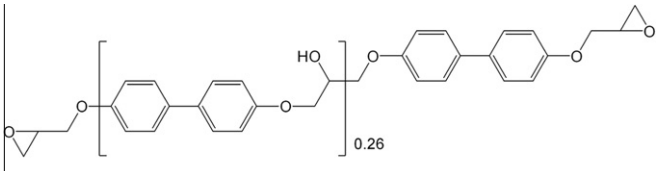

4, 4'-bis(2,3-epoxypropoxy) biphenyl epoxy resin

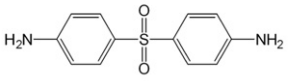

4, 4'-diaminodiphenylsulfone

Fig. 1 – Chemical structures of BP and DDS.

of the CNTs, first with a mixture of acids, then with LC epoxide functional groups for composite fabrication. The acid washing procedure removes amorphous carbon and impurities left from the CNT fabrication process, and at the same time induces some structural destruction to shorten the CNTs and create reactive sites on the surface of CNTs for the carboxylic groups to anchor on. Functionalizied nanotubes with LC epoxy resin encourage covalent bonding between the tubes and the epoxy resin and enhance the interfacial interaction for more ordered nanostructure. Surface modifications of CNTs were evaluated by TEM and characterized by using Fourier transform infrared spectroscopy (FTIR).

The FTIR spectra of p-CNT, a-CNT and ef-CNT are shown in Fig. 2 and the variation of absorption peaks have been discussed in our previous study [26]. These peaks are similar to those reported in previous literatures [29,30]. The presence of the epoxide ring peak implies that only part of the epoxy rings are opened and reacted, allowing for subsequent curing reaction.

The effects of the treatment on surface morphology can be detected by TEM. A very smooth surface can be observed on p-CNT (Fig. 3(a)) while a rough and damaged surface is shown on a-CNT (Fig. 3(b)). After a-CNT reacts with BP epoxy resin, the BP warps up and covers the CNTs and results in smoother surface than the acid-treated ones, as shown in Fig. 3(c).

The effect of functionalizing CNT on dispersion can be viewed in Fig. 4. After sonication, p-CNT still exhibits aggregation in water while a-CNT has increased dispersion. Furthermore, ef-CNT can be dispersed in THF much better than a-CNT after sonication as shown in Fig. 4(c) and (d). The epoxide groups attached to the CNTs create a barrier and debundle the gathered CNT. Concurrently, these epoxide groups increase the polarity of the tubes and hence increase the dispersion of the CNT in THF, which is a polar solvent. The functionalization of CNTs with LC epoxy resin not only efficiently achieves homogeneous dispersion but also increases the ordering morphology of composite which will be discussed in the following section.

3.3. *Morphology study of the composite of LC epoxy resin/CNT*

CNTs nucleating polymer during crystallization has been reported in CNTs/isotactic polypropylene (iPP) composite.

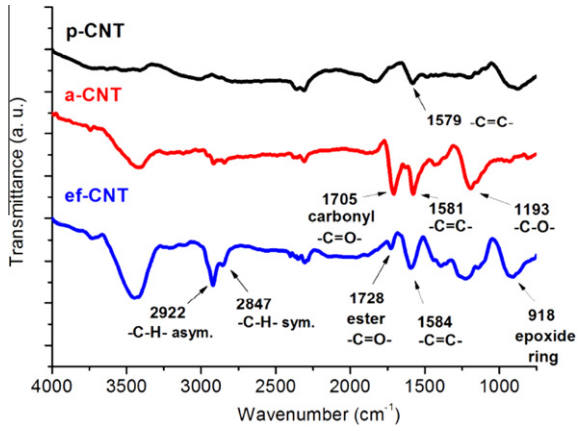

Fig. 2 – FTIR spectra of p-CNT, a-CNT and ef-CNT.

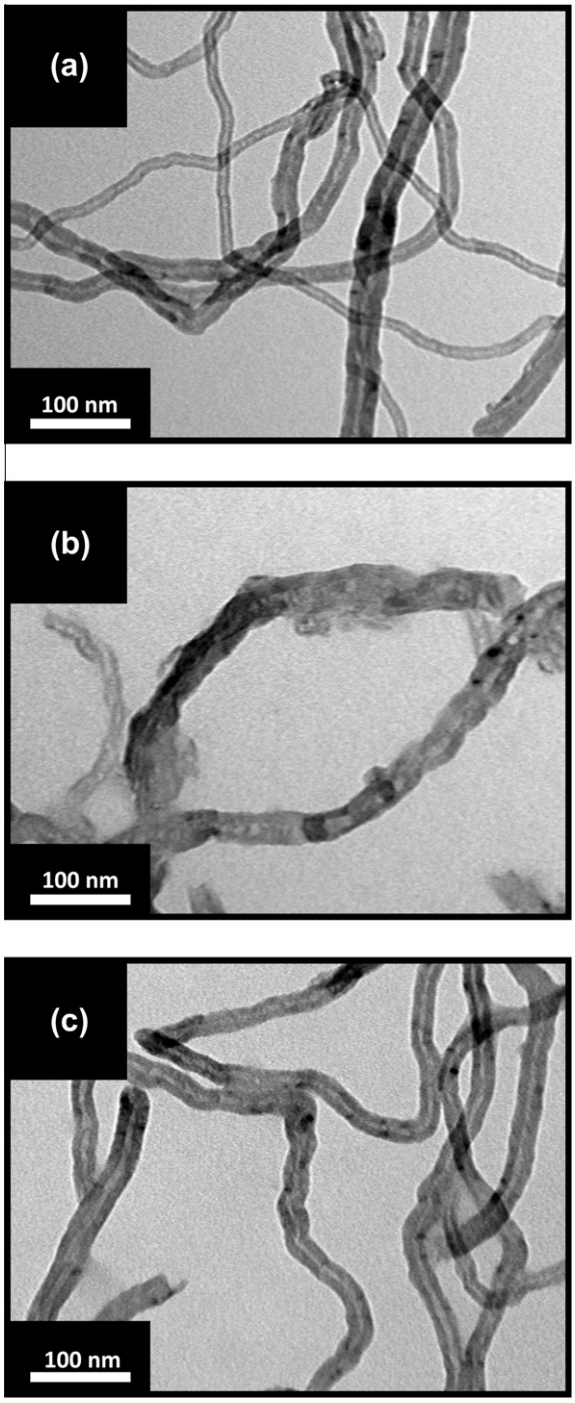

Fig. 3 – TEM images of: (a) p-CNT, (b) a-CNT and (c) ef-CNT.

The iPP crystals form a transcrystalline layer of aligned iPP lamellar crystals around the nucleating CNT [5]. For in situ polymerized CNTs/polyaniline (PANI) composite, the new ordered structure of PANI has been induced due to the CNTs nucleating cores and aniline monomers aligning on the surface of the CNTs before the initiation of polymerization. And thus, both the electrical conductivity, thermal stability have been improved due to the incorporation of CNTs [31]. In this study, we have observed the similar nucleating effect contributed by ef-CNT. The birefringence of the LC phase is clearly observed in the neat BP epoxy resin as shown in

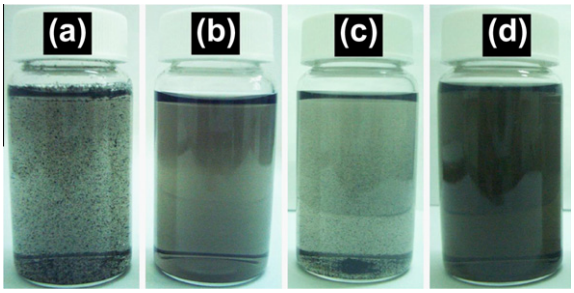

Fig. 4 – Effect of CNT functionalization on its dispersion: (a) p-CNT in water, (b) a-CNT in water, (c) a-CNT in THF, and (d) ef-CNT in THF.

Fig. 5(a). The 2.67 wt.% ef-CNT was dispersed in the BP resin and then cured with an equivalent DDS to make 2.00 wt.% ef-CNT/BP/DDS composite. When the BP epoxy resin containing 2.67 wt.% ef-CNT is heated to the LC temperature of BP epoxy resin (162 °C), the liquid crystal phase appears to grow toward a certain direction and induce an anisotropic crystallization. The micro-sized LC phase with fibrous structure is formed as shown in Fig. 5(b). Fig. 5(c) shows the crystalline morphology of cured BP/DDS resin. Its crystalline size is much smaller than that of neat BP epoxy resin due to the presence of DDS. The radially aligned morphology of BP/DDS resin indicates the crystalline is assembled along a certain direction. By adding ef-CNT in BP/DDS resin system results in the formation of long, straight and fibrous crystalline in a film sample, as shown in Fig. 5(d). Confining ef-CNT/BP/DDS between two glasses makes film sample devoid of spherical crystalline. The spherical crystalline (Fig. 5(e)) and the fibrous crystalline along with the spherical crystalline (Fig. 5(f)) are observed on the top surface and the fracture surface of ef-CNT/BP/DDS bulk sample respectively. We propose that during the curing process, the fibrous crystalline initially forms (Fig. 5(d)) and then grows into large spherical crystalline in the bulk sample (Fig. 6(a)).

The morphology of the cured ef-CNT/BP/DDS composite was investigated further by using SEM and TEM. For 2.00 wt.% ef-CNT/BP/DDS composite sample, the SEM image of the composite shows a large spherical crystalline structure that grows out of the fine crystalline structure (Fig. 6(a)) which is similar to what is observed in Fig. 5(f). Fig. 6(b), the

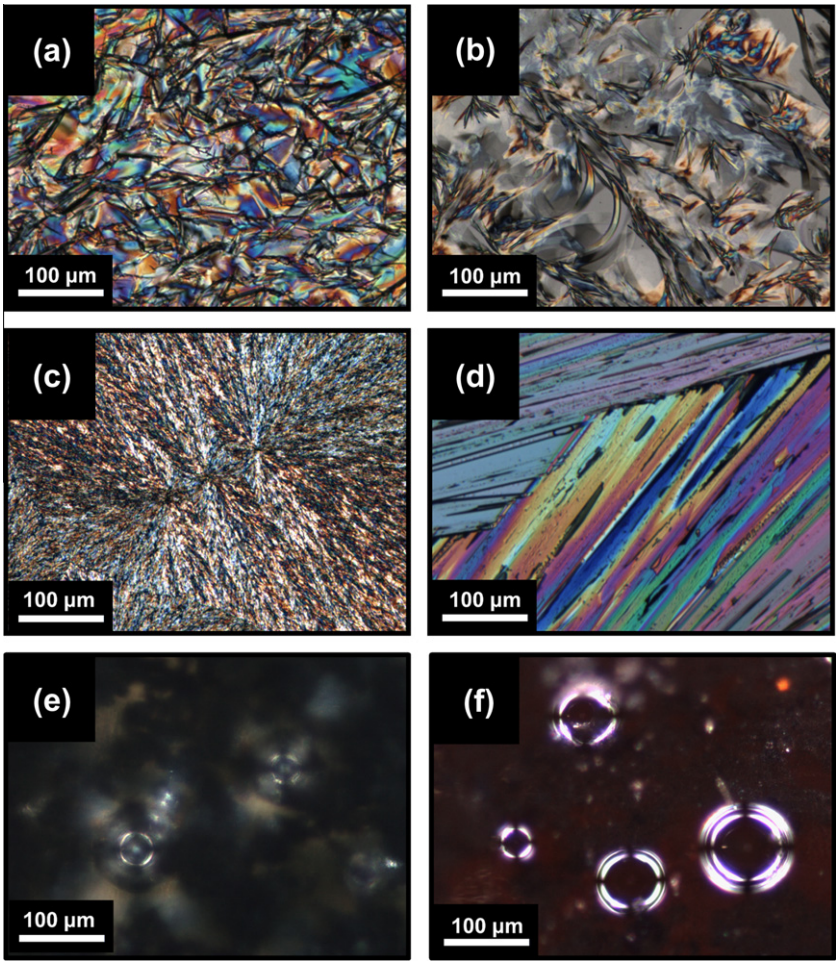

Fig. 5 – POM images of: (a) LC phase of BP epoxy resin, (b) crystalline of 2.67 wt.% ef-CNT/BP, (c) cured BP/DDS resin system, (d) cured thin film of 2.00 wt.% ef-CNT/BP/DDS, (e) the top view and (f) fracture surface of cured 2.00 wt.% ef-CNT/BP/DDS composite bulk sample.

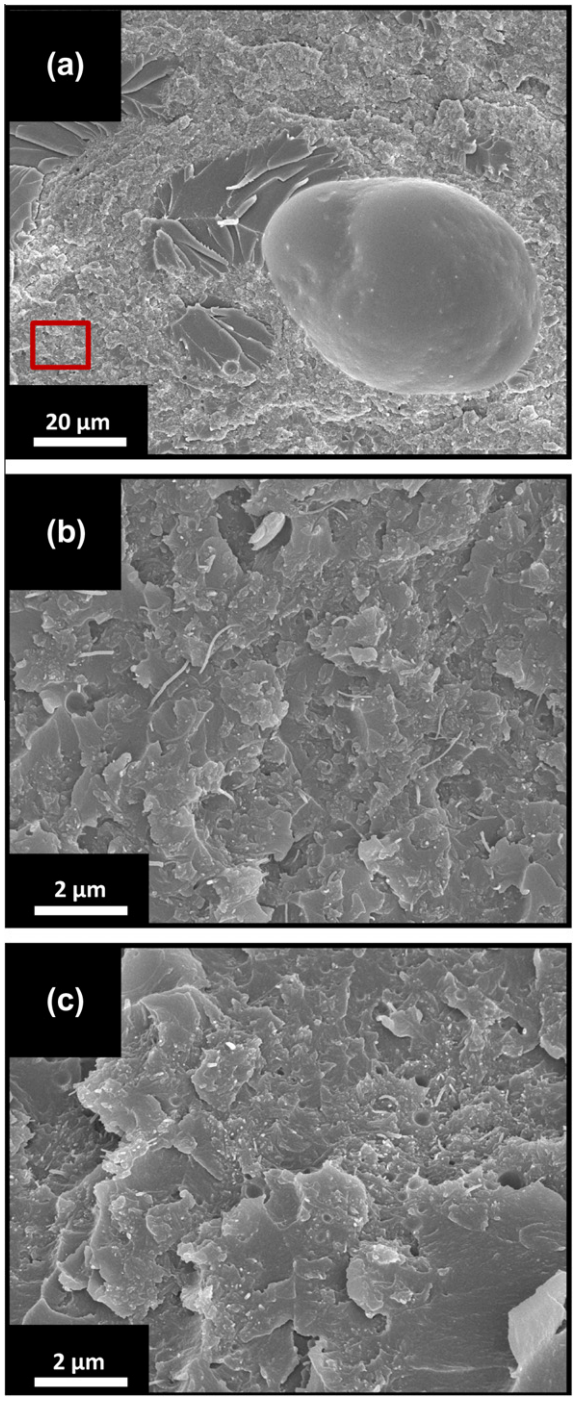

Fig. 6 – SEM images of: (a) the fracture surface, (b) higher magnification of the red** square area of the fracture surface of cured 2.00 wt.% ef-CNT/BP/DDS composite and (c) the fracture surface of 10.00 wt.% ef-CNT/BP/DDS composite. (For interpretation of the references to color in this figure legend, the reader is referred to the web version of this article.)**

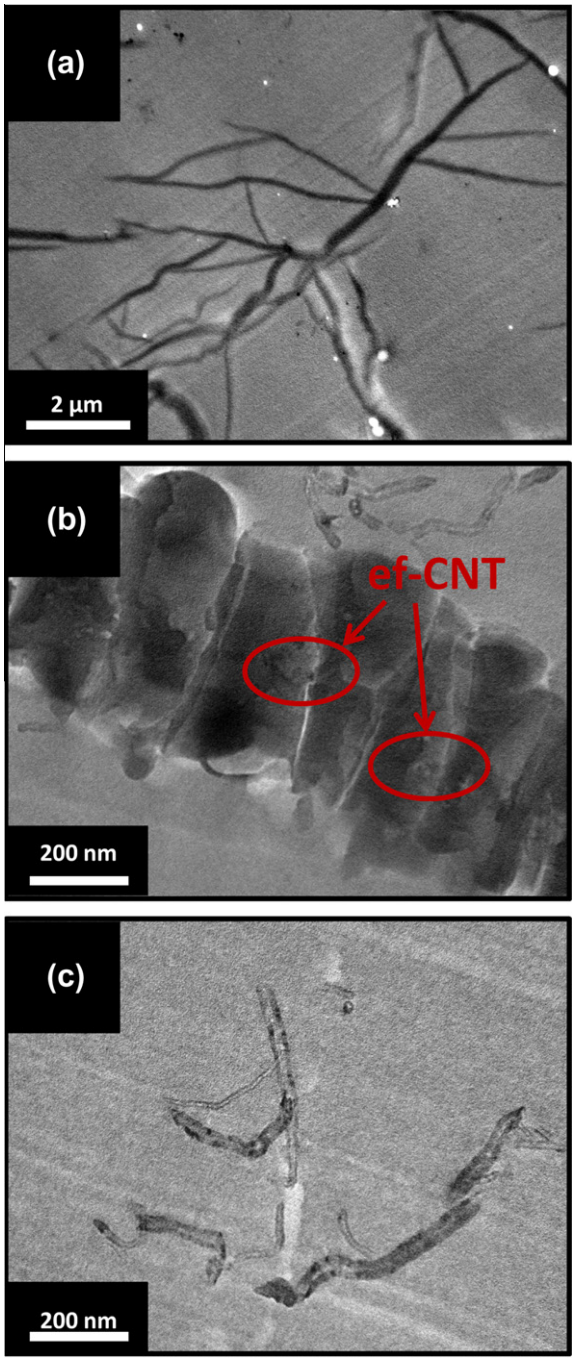

Fig. 7 – TEM images of: (a) branch structures, (b) higher magnification of branch structures, and (c) isolated ef-CNT in ef-CNT/BP/DDS composite. The presence of ef-CNT in the composite is pointed out by red circles in (b). (For interpretation of the references to color in this figure legend, the reader is referred to the web version of this article.)

enlargement of the fine crystalline area (red*** square of Fig. 6(a)) can tell the nanotubes are debundled, embedded and distributed throughout the matrix demonstrating effective functionalization and strong interaction between CNT and LC epoxy matrix. However, Fig. 6(c) shows the aggregates of ef-CNT in 10.00 wt.% ef-CNT/BP/DDS composite, which demonstrates CNTs tend to be entangled at higher concentration. Thus, a phase separation is occurred which lowers the mechanical strength of the composite at 10.00 wt.% ef-CNT loading. For the TEM study, 2.00 wt.% ef-CNT loading samples were used. Large branch structures are observed in the TEM

image as shown in Fig. 7(a). Under the higher magnification, Fig. 7(b) demonstrates that the crystalline structures are formed by the LC epoxy resin with ef-CNTs wrapped inside the crystal. This suggests that the branch structures of wrapped ef-CNTs act as the nuclei for growing fibrous crystalline and then eventually spherical crystalline. Meanwhile, few isolated ef-CNT (Fig. 7(c)) are also observed in the ef-CNT/BP/DDS composites indicating that the nucleating is not formed simultaneously throughout the matrix. Nevertheless, the incorporation of high thermal conductivity ef-CNT into matrix affords local nanoscale heating and formation of nucleating branches for the crystallization and accelerates the curing of ef-CNT/BP/DDS composite as well [26].

3.4. *Thermal properties of ef-CNT/LC epoxy composites*

With the incorporation of CNTs, the thermal properties of the LC epoxy resin are greatly improved. This observation is supported by TMA, DMA and TGA investigations.

Thermomechanical analysis (TMA) is a sensitive instrument which can measure the dimensional changes at micro-scale. Two transition points as glass transitions temperatures ($_{TMA}T_{g1}$ and $_{TMA}T_{g2}$) are observed in the curves shown in Fig. 8(a). Both $_{TMA}T_{g1}$ and $_{TMA}T_{g2}$ of ef-CNT/BP/DDS composites are calculated and listed in column 2 and the column 3 of Table 1, respectively. These two transitions imply that the reaction is a two-stage cure for the primary and secondary amines of DDS. The transitions are minor in the low ef-CNT concentration samples. However, for the samples with ef-CNT loading greater than 2.00 wt.%, the effect of ef-CNT addition on the degree of cure is dramatic since the polymer molecules are limited by an antedated vitrification and the physical presence of CNTs. In TMA analysis, both $_{TMA}T_{g1}$ and $_{TMA}T_{g2}$ increase from 191.3 and 204.6 °C for the neat epoxy resin, to 224.7 and 238.7 °C, respectively, with an increasing ef-CNT to 2.00 wt.%. The T_g increases because ef-CNT helps to immobilize the epoxy resin by holding the molecules together with strong interfacial interactions of relatively rigid ef-CNT. However, T_g decreases in higher ef-CNT concentrations because the high thermal conductivity of the CNTs accelerates the curing reaction to vitrification and results in a lower degree of conversion. The presence of uncured resin decreases the T_g of the composite. A detailed curing kinetic study of this composite has been reported in elsewhere [26].

The storage modulus and loss modulus properties of the composite are examined by DMA. In order to test the storage modulus at the exact same temperature for all the samples, the test begins at 50 °C instead of the room temperature. The storage modulus at 50 °C and the glass transition temperature ($_{DMA}T_g$) of the cured composites are shown in Fig. 8(b) and (c) with summarized results in column 4 of Table 1, respectively. Since the mechanical properties of reinforced composite strongly depend on the load transfer efficiency between the matrix and the reinforcement, functionalized CNTs are expected to strongly influence the elastic properties of the epoxy resin matrix. The storage modulus reveals that the amount of elastic energy stored in the composite is correlated to the mechanical properties and geometry of the reinforcement, the interfacial bonding characteristics, composite

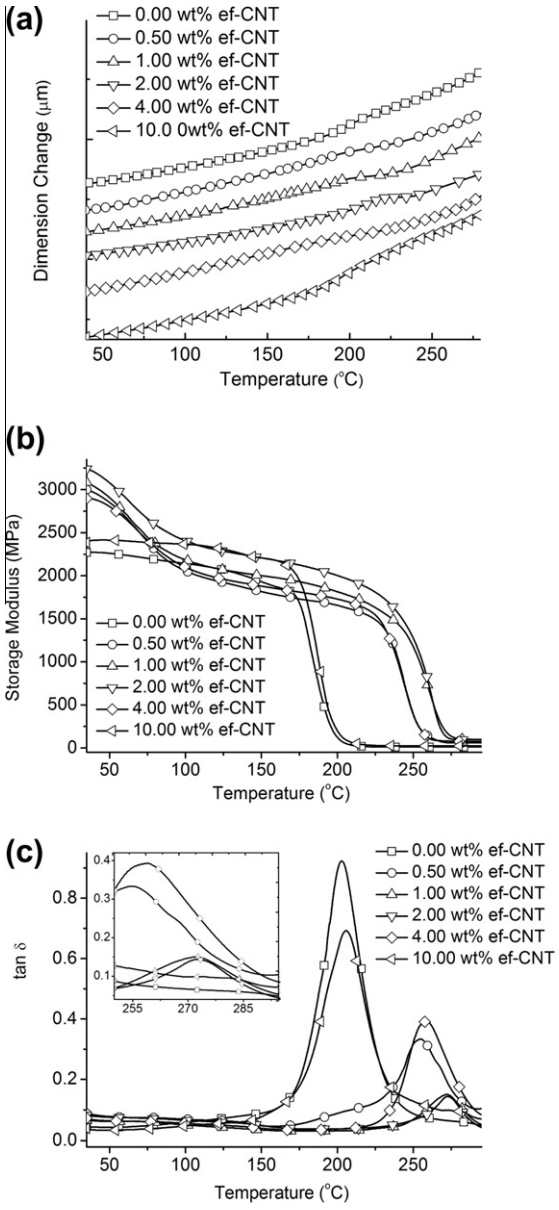

Fig. 8 – (a) TMA thermographs of bulk ef-CNT/BP/DDS composites, (b) storage modulus and (c) ratio of loss modulus to storage modulus (tan δ) of ef-CNT/BP/DDS composites obtained by DMA. The inset in (c) shows an enlargement of tan δ vs. Temperature at the temperature range of 250–295 °C.

morphology and the reinforcement composition. The neat epoxy resin has a storage modulus of 2.27 GPa and it is strengthen to 3.20 GPa, a 40.89% improvement, by 2.00 wt.% ef-CNT incorporation. This improvement results from the extremely high moduli of CNTs and their positive interactions with the polymer matrix. From Fig. 8(c), we can also see that the thermal stability of the composite is greatly improved. The tan δ (tan delta) is calculated from the ratio of loss modulus to storage modulus and the maximum peak position of tan δ is an indication of the glass transition temperature ($_{DMA}T_g$) of the composites. The $_{DMA}T_g$ of ef-CNT/BP/DDS

Table 1 – Summary of thermal and mechanical properties of ef-CNT/BP/DDS composites.

wt.% of ef-CNT	Properties						
	$_{TMA}T_{g1}$ (°C)	$_{TMA}T_{g2}$ (°C)	$_{DMA}T_{g}$ (°C)	Storage modulus at 50 °C (GPa)	T_d (°C)	Residual at 600 °C (wt.%)	Hardness [Hv(±SD)]
0.00	191.30	204.59	202.91	2.27	347.94	29.28	16.62(0.48)
0.50	196.79	230.70	254.86	2.96	358.44	26.60	20.99(0.50)
1.00	204.81	229.44	271.94	3.04	354.34	28.15	24.52(0.80)
2.00	224.71	238.65	272.87	3.20	361.71	29.09	27.14(1.22)
4.00	201.33	245.67	258.61	2.89	357.89	32.19	27.86(2.20)
10.00	184.01	241.63	205.91	2.41	357.94	37.20	28.02(1.80)

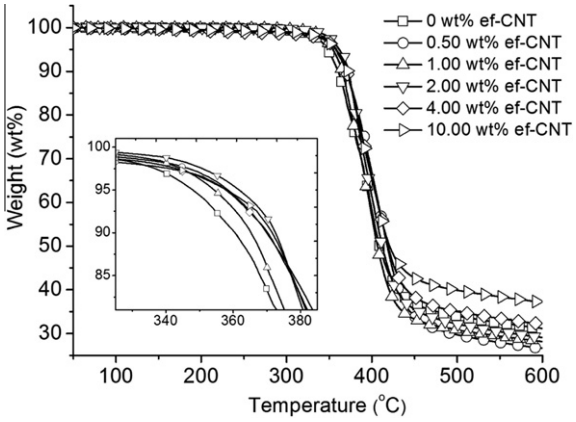

Fig. 9 – TGA thermographs of bulk ef-CNT/BP/DDS composites at different ef-CNT loading.

composites is raised from 202.91 °C for neat BP/DDS resin to 272.87 °C, with a 70.0 °C difference, after 2.00 wt.% ef-CNT is added into the composite. The improvement in $_{DMA}T_g$ is mainly attributed to the immobilization of reinforced LC epoxy resin through the formation of chemical bonding between the resin and functionalized CNT. Meanwhile, the amplitude of the tan δ peak is reduced, suggesting again that thermal stability is significantly enhanced since the polymer chain mobility is constrained even at high temperature. The mechanical properties of the composite are indeed enhanced by the incorporation of CNTs. Notice that 10.00 wt.% ef-CNT/BP/DDS displays the similar storage and loss modulus behaviors to those of neat BP/DDS resin. The result is due to the formation of aggregates of ef-CNT (see Fig. 6(c)) and fast reaching the vitrification stage of curing reaction. Thus, the reinforcing effect from ef-CNT and the degree of conversion of composite resin are constrained.

Thermal stability of the composites can be investigated by TGA and the results are shown in Fig. 9. The decomposition temperature (T_d) of the composite is determined at 5% weight loss and listed in Table 1. The T_d of the neat epoxy resin is 347.94 °C and is increased with an increasing of ef-CNT composition up to 2.00 wt.%. For the 0.50 wt.% ef-CNT sample, the decomposition temperature reaches 361.71 °C. Others researchers have shown an obvious increase in the T_d of CNTs/polymer composites after incorporating small amount of CNTs. However, progressively increasing the CNT percentage in polymer matrices results in an irregular increasing trend of T_d [32–34]. This phenomenon could arise from the enhanced thermal conductivity that is contributed by the increased amount of CNTs [26]. The functionalization of CNT substantially increases the interfacial bonding between the matrix and the reinforcement, efficiently reinforcing it to form a firm structure that is thermally stable. However, the T_d is decreased when the content of ef-CNT is higher than 2.00 wt.%. 10.00 wt.% ef-CNT sample has a T_d of only 357.94 °C, because the accelerated curing reaction vitrifies the matrix and decreases the curing conversion of the composites as described above. It is interesting to note that the residue amounts of the low ef-CNT concentration (< 2.00 wt.%) composite are lower than that of the neat epoxy resin (Table 1 column 7). The high thermal conductivity of CNTs may promote thermal decomposition of resin that is adjacent to them. As more ef-CNT is added into the composite, the extent of decrease is lowered due to an increase in the amount of thermal stable carbon.

3.5. *Mechanical properties of ef-CNT/LC epoxy composites*

The mechanical property of the composites is studied using a microhardness test (Table 1 column 8). When materials have higher crystallinity or are orderly arranged, their hardness increases. Also, adding reinforcement into an epoxy matrix increases the hardness of composite. The Vickers hardness of the neat epoxy resin is only 16.62 ± 0.47, while the condensed MWCNT film has a Vickers hardness of 9.2 ± 1.3 [35]. The hardness improves to 27.14 ± 1.22 Hv (a 63.3% increase as compared with cured BP/DDS resin system) when the content of ef-CNT is 2.00 wt.%. Since CNTs are resilient materials, homogeneously dispersed CNTs can add rigidity and hardness via interfacial interaction with the polymer matrix. Thus, the soft polymer matrix holds together when challenged by an applied force and the mechanical properties are improved. Another reason for the increase in hardness is that ef-CNT induces long range alignment of LC epoxy resin to forming the fibrous domains of high crystallinity. Higher ef-CNT concentrations (>2.00 wt.%) affects the curing reaction and attenuates any strengthening effects that usually result from ef-CNT.

4. Conclusions

MWCNT/LC epoxy composite was prepared using LC epoxy functionalized MWCNT. The composite exhibits significantly

enhanced physical properties. Successful functionalization of CNTs disrupts the strong van der Waals force between the nanotubes, preventing them from bundling together. Moreover, the BP epoxy resin grafted on ef-CNT increases the interfacial interaction between the nanotubes and the epoxy resin, increasing dispersion within the matrix. Due to the good interfacial interaction, the force applied on the matrix can be transferred to the nanotubes with improved thermal and mechanical properties. The LC epoxy resin molecules tend to align along the CNTs, resulting in an increase in the crystalline domain. Therefore, the ordered structures further improve the mechanical properties of the CNTs reinforced LC epoxy resins composite. Composites with 2.00 wt.% ef-CNT give the best overall performance among the composites. Since CNTs are found to influence the curing process and affect the crosslinking of the epoxy resins, higher compositions of ef-CNT do not give better performance. The addition of ef-CNT into the LC epoxy resin induces the formation of large LC domains and thus, the performance of composite is enhanced. This research provides an alternative novel material for strong and light-weight structural applications.

Acknowledgements

We thank National Science Council of Taiwan (NSC 99-2221-E-002-020-MY3) and Spirit Aerosystem Inc. USA for financial support. We also thank both Ms. Hao-Yueh Lo, M.S. Ed. in TESOL, University of Pennsylvania and Ms. Pauline Che, M.S. Eng. in BME, Johns Hopkins University for helping preparation and language check of this manuscript. The final grammar and language check for revision carried out by Mr. Anjey Su of Duquesne University, Pittsburgh, PA is highly appreciated.

REFERENCES

[1] Ajayan PM, Tour JM. Materials science – nanotube composites. Nature 2007;447(7148):1066–8.
[2] Tasis D, Tagmatarchis N, Bianco A, Prato M. Chemistry of carbon nanotubes. Chem Rev 2006;106(3):1105–36.
[3] Liu TX, Phang IY, Shen L, Chow SY, Zhang WD. Morphology and mechanical properties of multiwalled carbon nanotubes reinforced nylon-6 composites. Macromolecules 2004;37(19):7214–22.
[4] Koval'chuk AA, Shchegolikhin AN, Shevchenko VG, Nedorezova PM, Klyamkina AN, Aladyshev AM. Synthesis and properties of polypropylene/multiwall carbon nanotube composites. Macromolecules 2008;41(9):3149–56.
[5] Lu KB, Grossiord N, Koning CE, Miltner HE, van Mele B, Loos J. Carbon nanotube/isotactic polypropylene composites prepared by latex technology: morphology analysis of CNT-Induced nucleation. Macromolecules 2008;41(21):8081–5.
[6] Dombovari A, Halonen N, Sapi A, Szabo M, Toth G, Maklin J, et al. Moderate anisotropy in the electrical conductivity of bulk MWCNT/epoxy composites. Carbon 2010;48(7):1918–25.
[7] Iijima S. Helical microtubes of graphtic carbon. Nature 1991;354(6348):56–8.
[8] Ajayan PM. Nanotubes from carbon. Chem Rev 1999;99:1787–99.
[9] Zhang M, Fang SL, Zakhidov AA, Lee SB, Aliev AE, Williams CD, et al. Strong, transparent, multifunctional, carbon nanotube sheets. Science 2005;309(5738):1215–9.
[10] Paiva MC, Zhou B, Fernando KAS, Lin Y, Kennedy JM, Sun YP. Mechanical and morphological characterization of polymer-carbon nanocomposites from functionalized carbon nanotubes. Carbon 2004;42(14):2849–54.
[11] Schadler LS, Giannaris SC, Ajayan PM. Load transfer in carbon nanotube epoxy composites. Appl Phys Lett 1998;73(26):3842–4.
[12] Cooper CA, Young RJ, Halsall M. Investigation into the deformation of carbon nanotubes and their composites through the use of Raman spectroscopy. Compos Part A-Appl S 2001;32(3–4):401–11.
[13] Puglia D, Valentini L, Kenny JM. Analysis of the cure reaction of carbon nanotubes/epoxy resin composites through thermal analysis and Raman spectroscopy. J Appl Polym Sci 2003;88(2):452–8.
[14] Xie HF, Liu BH, Yuan ZR, Shen JY, Cheng RS. Cure kinetics of carbon nanotube/tetrafunctional epoxy nanocomposites by isothermal differential scanning calorimetry. J Polym Sci Polym Phys 2004;42(20):3701–12.
[15] Su WFA. Thermoplastic and thermaoset main-chain liquid-crystal polymer prepared from biphenyl mesogen. J Polym Sci Polym Chem 1993;31(13):3251–6.
[16] Su WFA, Schoch KF, Smith JDB. Comparison of cure conditions for rigid rod epoxy and bisphenol a epoxy using thermomechanical analysis. J Appl Polym Sci 1998;70(11):2163–7.
[17] Barclay GG, Ober CK, Papathomas KI, Wang DW. Liquid-crystalline epoxy thermosets based on dihydroxymethylstilbene – synthesis and characterization. J Polym Sci Polym Chem 1992;30(9):1831–43.
[18] Su WFA, Chen KC, Tseng SY. Effects of chemical structure changes on thermal, mechanical, and crystalline properties of rigid rod epoxy resins. J Appl Polym Sci 2000;78(2):446–51.
[19] Mititelu-Mija A, Cascaval CN. Liquid crystalline epoxy azomethine thermoset. High Perform Polym 2007;19(2):135–46.
[20] Harada M, Sumitomo K, Nishimoto Y, Ochi M. Relationship between fracture toughness and domain size of liquid-crystalline epoxy resins having polydomain structure. J Polym Sci Polym Phys 2009;47(2):156–65.
[21] Harada M, Watanabe Y, Tanaka Y, Ochi M. Thermal properties and fracture toughness of a liquid-crystalline epoxy resin cured with an aromatic diamine crosslinker having a mesogenic group. J Polym Sci Polym Phys 2006;44(17):2486–94.
[22] Harada M, Ochi M, Tobita M, Kimura T, Ishigaki T, Shimoyama N, et al. Thermal-conductivity properties of liquid-crystalline epoxy resin cured under a magnetic field. J Polym Sci Polym Phys 2003;41(14):1739–43.
[23] Harada M, Akamatsu N, Ochi M, Tobita M. Investigation of fracture mechanism on liquid crystalline epoxy networks arranged by a magnetic field. J Polym Sci Polym Phys 2006;44(10):1406–12.
[24] Harada M, Ochi M, Tobita M, Kimura T, Ishigaki T, Shimoyama N, et al. Thermomechanical properties of liquid-crystalline epoxy networks arranged by a magnetic field. J Polym Sci Polym Phys 2004;42(5):758–65.
[25] Bae J, Jang J, Yoon SH. Cure Behavior of the liquid-crystalline epoxy/carbon nanotube system and the effect of surface treatment of carbon fillers on cure reaction. Macromol Chem Phys 2002;203(15):2196–204.
[26] Chen S, Hsu S-H, Wu M-C, Su W-F. Kinetics studies on the accelerated curing of liquid crystalline epoxy resin/multi-walled carbon nanotube nanocomposites. J Polym Sci B Polym Phys 2011;49(4):301–9.

[27] Lee H, Neville K. Handbook of epoxy resins. 1st ed. New York: McGraw-Hill; 1967.
[28] Zhu J, Kim JD, Peng HQ, Margrave JL, Khabashesku VN, Barrera EV. Improving the dispersion and integration of single-walled carbon nanotubes in epoxy composites through functionalization. Nano Lett 2003;3(8):1107–13.
[29] Zhu J, Peng HQ, Rodriguez-Macias F, Margrave JL, Khabashesku VN, Imam AM, et al. Reinforcing epoxy polymer composites through covalent integration of functionalized nanotubes. Adv Funct Mater 2004;14(7):643–8.
[30] Wang S, Liang R, Wang B, Zhang C. Reinforcing polymer composites with epoxide-grafted carbon nanotubes. Nanotechnology 2008;19(8):085710.
[31] Feng W, Bai XD, Lian YQ, Liang J, Wang XG, Yoshino K. Well-aligned polyaniline/carbon-nanotube composite films grown by in-situ aniline polymerization. Carbon 2003;41(8):1551–7.
[32] Xia HS, Song M. Preparation and characterisation of polyurethane grafted single-walled carbon nanotubes and derived polyurethane nanocomposites. J Mater Chem 2006;16(19):1843–51.
[33] Kuan HC, Ma CCM, Chang WP, Yuen SM, Wu HH, Lee TM. Synthesis, thermal, mechanical and rheological properties of multiwall carbon nano tube/waterborne polyurethane nanocomposite. Compos Sci Technol 2005;65(11–12): 1703–10.
[34] Kodjie SL, Li LY, Li B, Cai WW, Li CY, Keating M. Morphology and crystallization behavior of HDPE/CNT nanocomposite. J Macromol Sci B 2006;45(2):231–45.
[35] Ogino SI, Sato Y, Yamamoto G, Sasamori K, Kimura H, Hashida T, et al. Relation of the number of cross-links and mechanical properties of multi-walled carbon nanotube films formed by a dehydration condensation reaction. J Phys Chem B 2006;110(46):23159–63.